



Research Papers

## Detecting time-averaging and spatial mixing using oxygen isotope variation: a case study

David H. Goodwin<sup>a,\*</sup>, Karl W. Flessa<sup>a</sup>, Miguel A. Téllez-Duarte<sup>b</sup>,  
David L. Dettman<sup>a</sup>, Bernd R. Schöne<sup>a,1</sup>, Guillermo A. Avila-Serrano<sup>b</sup>

<sup>a</sup>Department of Geosciences, University of Arizona, Tucson, AZ 85721, USA

<sup>b</sup>Facultad de Ciencias Marinas, Universidad Autónoma de Baja California, Ensenada, Baja California, Mexico

Received 22 July 2002; received in revised form 29 April 2003; accepted 6 October 2003

### Abstract

In principle, bivalve mollusks living at the same time and in the same place will experience the same temperature and salinity regimes and will have identical annual oxygen isotope ( $\delta^{18}\text{O}$ ) profiles. Bivalve mollusks living at different times or in different places are more likely to have different annual  $\delta^{18}\text{O}$  profiles. Thus, differences in annual  $\delta^{18}\text{O}$  profiles can be used to detect temporal or spatial mixing.

We devised eight metrics to quantitatively compare sclerochronologically calibrated annual  $\delta^{18}\text{O}$  profiles from different shells: difference in maximum value, difference in minimum value, difference in amplitude, the number of non-contemporaneous isotopic enrichment events (NNEE), the average fortnightly difference (AD), the standard deviation of the average fortnightly differences (SDD), the maximum fortnightly difference (MaxD) and the number of fortnights separating the minimum values.

These metrics vary among northern Gulf of California shells from four temporal and spatial categories: (1) same time and same place; (2) same time and different place; (3) different time and same place; and (4) different time and different place. Different time/different place comparisons include comparisons of live-collected shells with shells alive during times of Colorado River flow and shells from a Pleistocene interglacial deposit. The same time/same place comparison has the most similar metric values, whereas comparisons among the different time/different place shells are usually the least similar.

Between-shell oxygen isotope differences can reveal temporal or spatial mixing of shells that would be undetectable with radiocarbon or amino-acid racemization dating. Application of the technique to a Holocene deposit with shells in life position reveals that the bivalves were alive at different times, despite indistinguishable radiocarbon ages. Two adjacent but disarticulated Pleistocene shells appear to be both temporally and spatially mixed. The method can detect temporal or spatial mixing in any shell material unaffected by diagenesis, regardless of the age of the specimens.

© 2004 Published by Elsevier B.V.

**Keywords:** Taphonomy; Time-averaging; Spatial-mixing; Oxygen isotopes; Gulf of California; Mollusks

\* Corresponding author. Current address: Department of Geology and Geography, Denison University, F.W. Olin Science Hall, Granville, OH, 43023, USA. Tel.: +1-740-587-5621; fax: +1-740-587-6774.

E-mail address: [goodwind@denison.edu](mailto:goodwind@denison.edu) (D.H. Goodwin).

<sup>1</sup> Current address: Institute and Museum for Geology and Paleontology, Johann Wolfgang Goethe University, Senckenberganlage 32-34, 60054 Frankfurt am Main, Germany.

## 1. Introduction

Time-averaging and spatial-mixing limit our ability to faithfully reconstruct the past by blurring the record of environmental and ecological conditions (Fürsich and Aberhan, 1990). Time-averaged and spatially mixed deposits represent the sum of community composition and structure, during some interval, over some area (Allison and Briggs, 1991; and references therein Kidwell and Behrensmeyer, 1993). Recognizing and evaluating the magnitude of time-averaging and spatial mixing is therefore essential for reconstructing ancient environments and ecological conditions.

Detecting time-averaging is particularly important when investigating deposits thought to represent ecological snapshots (*sensu* Kidwell and Bosence, 1991). Catastrophic burial of benthic communities can result in the preservation of a census assemblage. Such deposits are typically characterized by large numbers of articulated specimens preserved in life position. Census assemblages can preserve ecological information such as spatial relationships, size-frequency distributions and relative abundances (Kidwell and Bosence, 1991). However, interpretation of catastrophically buried communities may be complicated by the presence of dead individuals that persisted in life-position in the habitat at the time of burial (e.g., Iribarne et al., 1998). Thus, identification of such short-duration time-averaging is critical for the recognition and interpretation of census assemblages.

Many authors have suggested techniques for identifying and evaluating the extent of time-averaging (e.g., Kidwell and Bosence, 1991; Flessa, 1993, 2001; Behrensmeyer et al., 2000). One of the most common approaches involves estimating the age range of directly dated fossils contained within the unit (Flessa et al., 1993; Flessa and Kowalewski, 1994; Kowalewski et al., 1998), thereby establishing the magnitude of time-averaging. However, this method is limited, either by the amount of money available for dating or the range and precision of the direct-dating technique. Because the scale of time-averaging can be shorter than the error associated with direct-dating techniques (typically ~ 50 years), these techniques are insensitive to short-duration (<100 years) time-averaging.

Spatial mixing also confounds our ability to reconstruct and interpret ancient communities. Fortunately, out-of-habitat spatial mixing is generally thought to be a minor taphonomic phenomenon for macrofossils (Kidwell and Flessa, 1995; also see Behrensmeyer et al., 2000; Martin, 1999; and references therein), and can often be identified by the presence of exotic species, taphonomic conditions that suggest transportation, or by the depositional context. However, identifying within-habitat spatial mixing is a greater challenge. Miller (1988) and Springer and Flessa (1996) demonstrated that within-habitat faunal spatial distributions could be preserved in some circumstances. However, most fossil remains are probably reworked and scattered within their original habitat (Kidwell and Flessa, 1995). Because death assemblages often represent cumulative community structure over some area they may fail to capture small-scale spatial variability, such as patchiness and gradients within the habitat. Therefore, identifying within-habitat spatial mixing is essential for interpreting fossil assemblages.

Here, we present a new method to accomplish these goals based on geochemical variability in the shells of bivalve mollusks (e.g., Bianucci and Longinelli, 1982; Cespuglio et al., 1999; Keller et al., 2002). The basic idea is simple: clams that live in the same place at the same time will experience the same temperature and salinity regimes (Goodwin et al., 2001). Therefore, shells of organisms that grow in the same place (separated by a few meters) at the same time will have similar annual isotopic profiles, whereas shells of organisms that grew at different places and/or different times are likely to have different annual isotopic profiles. Consider annual oxygen isotope ( $\delta^{18}\text{O}$ ) profiles from shells from two hypothetical deposits, one containing shells that were not time-averaged or spatially mixed, the other containing time-averaged and/or spatially mixed shells. In the case of the non-mixed pair (Fig. 1A), the two shells have virtually identical annual isotopic profiles, reflecting the fact that the individuals grew in the same environmental conditions at the same time and place. In the second scenario (Fig. 1B), the two shells have different annual isotopic profiles. The difference between the two profiles suggests that the individuals did not experience the same environmental conditions and indicates that the deposit is time-averaged and/or spatially mixed.

To detect temporal and spatial mixing, we compare sclerochronologically calibrated, within-shell  $\delta^{18}\text{O}$  variation among bivalve mollusks collected from several localities in the northern Gulf of California (Fig. 2). The comparisons allow us to evaluate the differences in annual isotopic variation within and among the following temporal/spatial categories: (1) clams that lived at the same time in the same place; (2) clams that lived at the same time in different places; (3) clams that lived at different times in the same place; and (4) clams that lived at different times in different places. We devise eight metrics to measure the dissimilarity of annual isotope profiles and then assess the contributions of spatial and temporal mixing to differences in isotopic variation. Furthermore,

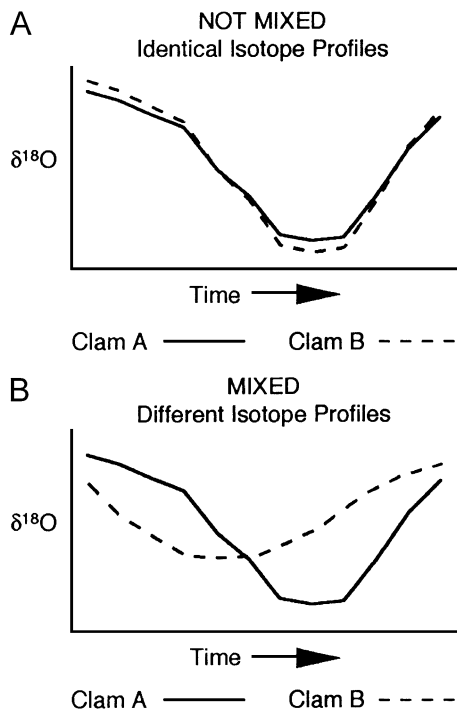


Fig. 1. Schematic illustration of the method for using annual oxygen isotopic profiles to detect time-averaging and spatial mixing. (A) Annual isotopic profiles from two shells in a deposit not affected by temporal or spatial mixing. In this example, shells alive at the same time in the same place have nearly identical annual isotopic profiles. (B) Annual isotopic profiles from shells in a temporally or spatially mixed deposit. Shells from this deposit lived at different times and/or different places and experienced different environmental conditions, resulting in different annual isotopic profiles.

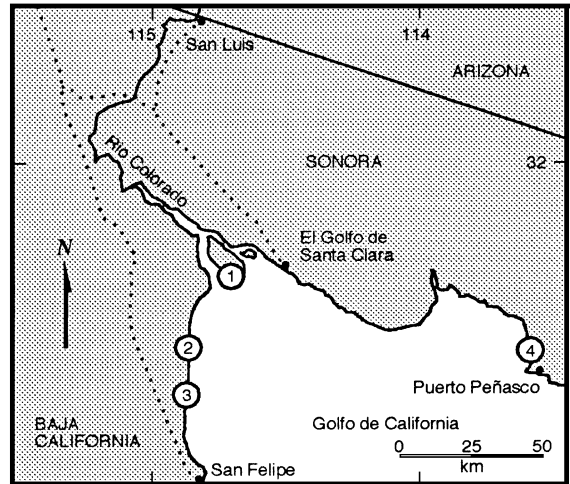


Fig. 2. Locality map of the study area. Shells were collected from four localities in the northern Gulf of California: (1) Isla Montague, (2) North Orca, (3) Campo Don Abel and (4) Bahia la Choya. See Table 1 for additional locality information and details on the shells used in this study.

in addition to identifying time-averaging and spatial mixing, the metrics can provide clues to the cause(s) of geochemical differences. We then apply our technique to shells from two deposits with unknown temporal and/or spatial affinities: (1) Holocene shells found articulated and in life-position, and (2) disarticulated shells from a last interglacial deposit (Marine Isotope Sub-stage 5e, ~ 125,000 ybp).

## 2. Materials and methods

Our study area (Fig. 2) in the northern Gulf of California experiences large seasonal changes in temperature, hot and arid conditions, and large amplitude tides. Average monthly summer temperatures exceed 32 °C and winter temperatures fall below 12 °C (Hastings, 1964a,b). Daily temperatures are more extreme than monthly averages. In 1999, our instruments in the intertidal zone recorded a maximum daily temperature of 40.6 °C and a minimum of 3.3 °C (Goodwin et al., 2001). The regional climate is extremely arid: average annual rainfall is between 60–75 mm (Hastings, 1964a,b). The northern Gulf of California experiences strong semi-diurnal tides with amplitudes up to 10 m (Thompson, 1968). The Colo-

rado River delta, located in the western half of the study area, is characterized by extensive tidal flats dominated by fine-grained sediments separated by shelly beach ridges or cheniers (Thompson, 1968). Since 1960, only a very limited amount of Colorado River water has reached the Gulf of California.

We use shells from two extant species of bivalve mollusks, *Chione cortezi* and *Chione californiensis*. Both species are shallow infaunal clams found in fine-sand and muddy sediments (Keen, 1971). Cross-calibration of stable oxygen isotope values with environmental variables indicates that during shell deposition these species fractionate oxygen isotopes in equilibrium with seawater (see Goodwin et al., 2001). *C. cortezi* and *C. californiensis* have shells composed exclusively of aragonite and reach a shell height of ~ 8 cm within 5–6 years (Schöne et al., 2002).

We collected four sets of shells, each from a different locality (Fig. 2, Table 1). The first two sets were live-collected specimens of *C. cortezi*. Two specimens, separated by ~ 2 m, were collected from the middle intertidal zone at Isla Montague in February 1999 (Fig. 2, Table 1). The second live-collected set is from the North Orca locality (Fig. 2, Table 1). Here, we recovered two clams from the high-intertidal zone and a third from the low-intertidal zone.

The final two sets of shells were collected dead. Three *C. cortezi* were collected dead, but articulated and in life position from the tide flats at Campo don Abel (Fig. 2, Table 1). Finally, two *C. californiensis* were collected from a Pleistocene terrace at Bahia la Choya (Fig. 2, Table 1). These shells were not

articulated or in life position. According to Aberhan and Fürsich (1991), these sandy to rocky deposits originated in the shallow, subtidal zone.

Comparisons of shells with known temporal and spatial relationships, both within and among sets, fall into four temporal/spatial categories (Table 2):

*Same time/same place*; (ST/SP). Only one comparison falls into this category: the two contemporaneous and adjacent shells from Isla Montague, IM11-A1L and IM11-A2L.

*Same time/different place*; (ST/DP). Only one comparison falls into this category: the two North Orca shells collected alive in 1998 (NO4-A2R and NO4-A3R). One is from the high intertidal zone; the other is from the low intertidal zone, approximately 1.5 km distant.

*Different time/same place*; (DT/SP). Four comparisons fit this category. Comparison of the two high intertidal shells collected from North Orca and comparisons of subsequent growth years within each of the three Campo don Abel shells. Note that, in these three comparisons, two annual profiles within the same shell are being compared. In these circumstances, the profiles are clearly from the same place because they are from the same specimen; they differ in time by 1 year.

*Different time/different place*; (DT/DP). Fifty-nine comparisons fit this category:

(a) Modern–Modern. Seven comparisons of the live-collected shells.

Table 1  
Specimen information for the shells used in this study

Shell ID	Latitude	Longitude	Age	Intertidal position	Growth interval sampled	# years sampled
IM11-A1L	31 40.22'	114 41.41'	live	middle	1999	one
IM11-A2L	31 40.22'	114 41.41'	live	middle	1999	one
NO4-A1R	31 20.75'	114 52.78'	live	high	~ 1993	one
NO4-A2R	31 20.75'	114 52.78'	live	low	1998	one
NO4-A3R	31 20.75'	114 52.78'	live	high	1998	one
DA4-D1R	31 11.93'	114 53.12'	354–530 (AA34415)	high?	NA	two
DA4-D3R	31 11.93'	114 53.12'	353–519 (AA40170)	high?	NA	two
DA4-D5R	31 11.93'	114 53.12'	350?–525?	high?	NA	two
CB(P)-3	31 21.10'	113 36.30'	~ 125 ka	NA	NA	one
CB(P)-4	32 21.10'	114 36.30'	~ 125 ka	NA	NA	one

Table 2

Metric values and principal component scores for all  $\delta^{18}\text{O}$  profile comparisons

	Comparison #	Shell 1	Shell 2	$D_{\max}$	$D_{\min}$	$D_{\text{amp}}$	NNEE	AD	SDD	MaxD	$T_{\min}$	PC1	PC2	PC3
	1	Identical		0.00	0.00	0.00	0	0.00	0.00	0.00	0	0.00	0.00	0.00
<i>Same time–same place (n=1)</i>														
	2	IM11-A1L	IM11-A2L	0.49	0.02	0.47	0	0.33	0.24	0.85	1	−1.14	0.30	−0.05
<i>Same time–different place (n=1)</i>														
	35	NO4-A2R	NO4-A3R	1.78	0.40	1.38	1	0.92	0.63	2.60	0	−2.81	−0.47	1.30
<i>Different time–same place (n=4)</i>														
	26	NO4-A1R	NO4-A3R	0.29	0.06	0.35	1	0.73	0.48	1.79	3	−2.37	0.11	−1.60
	65	DA4-D1R1	DA4-D1R2	0.01	0.60	0.61	1	2.55	1.30	4.30	7	−6.12	0.77	−3.88
	74	DA4-D3R1	DA4-D3R2	0.46	0.01	0.12	0	0.49	0.50	1.56	5	−2.54	1.26	−2.36
	79	DA4-D5R1	DA4-D5R2	0.14	0.40	0.26	1	0.29	0.30	1.21	1	−1.34	−0.58	−0.63
Group average				0.82	0.27	0.34	0.75	1.02	0.65	2.22	4.00			
<i>Different time–different place (n=59)</i>														
Modern– Modern (n=7)	3	NO4-A1R	IM11-A1L	1.43	0.01	1.14	3	1.32	0.82	2.54	5	−4.04	−0.66	−1.95
	4	NO4-A2R	IM11-A1L	0.64	0.35	0.29	3	0.91	0.57	1.95	8	−3.79	−0.31	−4.47
	5	NO4-A3R	IM11-A1L	1.14	0.05	1.09	1	0.75	0.66	2.15	8	−4.01	1.16	−3.25
	14	NO4-A1R	IM11-A2L	0.94	0.03	0.97	3	1.35	0.80	2.46	4	−3.63	−0.88	−1.99
	15	NO4-A2R	IM11-A2L	1.13	0.37	0.76	3	0.89	0.55	2.03	7	−3.76	−0.50	−3.42
	16	NO4-A3R	IM11-A2L	0.65	0.03	0.62	4	0.81	0.62	2.08	7	−3.59	−1.01	−4.07
	25	NO4-A1R	NO4-A2R	2.07	0.34	1.73	0	0.93	0.61	2.07	3	−3.27	0.73	0.46
Group average				1.14	0.17	0.94	2.43	0.99	0.66	2.18	6			
Modern– Holocene (n=30)	8	DA4-D1R1	IM11-A1L	0.39	1.63	2.02	3	1.15	0.72	2.38	0	−3.25	−3.05	0.46
	9	DA4-D1R2	IM11-A1L	0.39	1.03	1.41	2	1.79	0.78	2.67	7	−4.86	−0.50	−3.24
	10	DA4-D3R1	IM11-A1L	0.29	1.44	1.15	3	1.04	0.80	2.55	5	−4.02	−1.76	−2.64
	11	DA4-D3R2	IM11-A1L	0.18	1.45	1.27	3	1.42	0.70	2.22	0	−2.89	−2.83	−0.09
	12	DA4-D5R1	IM11-A1L	0.54	1.20	0.66	3	0.60	0.58	2.15	4	−3.13	−1.69	−2.24
	13	DA4-D5R2	IM11-A1L	0.40	0.80	0.40	2	0.71	0.57	1.66	3	−2.54	−1.00	−1.70
	19	DA4-D1R1	IM11-A2L	0.10	1.65	1.55	3	1.37	0.65	2.17	1	−3.13	−2.86	−0.45
	20	DA4-D1R2	IM11-A2L	0.11	1.05	0.94	2	1.86	0.75	2.93	6	−4.69	−0.63	−3.18
	21	DA4-D3R1	IM11-A2L	0.78	1.46	0.68	3	1.01	0.63	2.09	4	−3.44	−1.81	−2.07
	22	DA4-D3R2	IM11-A2L	0.67	1.47	0.80	3	1.40	0.72	2.54	1	−3.29	−2.39	−0.61
	23	DA4-D5R1	IM11-A2L	1.03	1.22	0.19	3	0.59	0.42	1.30	3	−2.36	−1.79	−1.64
	24	DA4-D5R2	IM11-A2L	0.89	0.82	0.07	4	0.71	0.42	1.36	2	−2.09	−2.38	−1.59
	29	DA4-D1R1	NO4-A1R	1.04	1.62	0.58	2	2.15	1.36	4.52	5	−6.02	−0.63	−2.49
	30	DA4-D1R2	NO4-A1R	1.05	1.02	0.03	1	1.03	0.63	2.15	2	−2.97	−0.38	−0.80
	31	DA4-D3R1	NO4-A1R	1.72	1.43	0.29	2	1.53	0.68	2.47	0	−3.14	−1.55	0.47
	32	DA4-D3R2	NO4-A1R	1.61	1.44	0.17	2	1.62	0.75	3.12	5	−4.63	−0.52	−2.23
	33	DA4-D5R1	NO4-A1R	1.97	1.19	0.78	2	1.35	0.70	2.26	1	−3.22	−1.28	0.39
	34	DA4-D5R2	NO4-A1R	1.83	0.79	1.04	3	1.27	0.61	2.13	2	−3.21	−2.61	−0.32
	38	DA4-D1R1	NO4-A2R	1.03	1.28	2.31	2	1.54	0.75	2.86	8	−5.35	−0.50	−2.85
	39	DA4-D1R2	NO4-A2R	1.02	0.68	1.70	1	1.15	0.66	2.54	1	−3.15	−0.71	0.57
	40	DA4-D3R1	NO4-A2R	0.35	1.09	1.44	2	0.73	0.45	1.52	3	−2.66	−1.47	−1.09
	41	DA4-D3R2	NO4-A2R	0.46	1.10	1.56	2	0.79	0.58	2.32	8	−4.32	−0.41	−3.55
	42	DA4-D5R1	NO4-A2R	0.10	0.85	0.95	2	0.68	0.53	2.10	4	−3.02	−0.99	−2.09
	43	DA4-D5R2	NO4-A2R	0.24	0.45	0.69	3	0.58	0.49	1.65	5	−2.80	−1.17	−2.91
	46	DA4-D1R1	NO4-A3R	0.75	1.68	0.93	1	1.88	1.05	3.87	8	−6.05	0.31	−3.61
	47	DA4-D1R2	NO4-A3R	0.76	1.08	0.32	2	1.47	0.90	3.15	1	−3.59	−1.26	−0.67
	48	DA4-D3R1	NO4-A3R	1.43	1.49	0.06	1	1.35	0.53	2.37	3	−3.51	−0.40	−1.04

(continued on next page)

Table 2 (continued)

	Comparison #	Shell 1	Shell 2	$D_{\max}$	$D_{\min}$	$D_{\text{amp}}$	NNEE	AD	SDD	MaxD	$T_{\min}$	PC1	PC2	PC3
<i>Different time–different place (n=59)</i>														
Modern–	49	DA4-D3R2	NO4-A3R	1.32	1.50	0.18	1	1.62	0.46	2.55	8	–4.81	0.51	–3.56
Holocene	50	DA4-D5R1	NO4-A3R	1.68	1.25	0.43	1	0.89	0.54	1.97	4	–3.31	–0.12	–1.18
(n=30)	51	DA4-D5R2	NO4-A3R	1.54	0.85	0.69	1	0.90	0.49	1.84	5	–3.37	0.21	–1.63
Group average				0.86	1.20	0.84	2.17	1.21	0.66	2.38	3.63			
Modern–	6	CB(P)-3	IM11-A1L	0.04	0.20	0.16	1	0.74	0.42	1.44	5	–2.56	0.35	–2.81
Pleistocene	7	CB(P)-4	IM11-A1L	0.64	0.02	0.62	3	0.61	0.43	1.38	6	–2.79	–0.64	–3.24
(n=10)	17	CB(P)-3	IM11-A2L	0.53	0.22	0.31	3	0.72	0.40	1.50	4	–2.44	–1.09	–2.46
	18	CB(P)-4	IM11-A2L	1.13	0.04	1.09	3	0.58	0.43	1.38	5	–2.72	–0.84	–2.18
	27	CB(P)-3	NO4-A1R	1.47	0.19	1.28	2	0.87	0.64	1.87	0	–2.28	–1.12	0.85
	28	CB(P)-4	NO4-A1R	2.07	0.01	2.06	2	1.10	0.71	2.09	1	–2.95	–0.83	1.09
	36	CB(P)-3	NO4-A2R	0.60	0.15	0.45	2	0.35	0.37	1.52	3	–2.05	–0.59	–1.58
	37	CB(P)-4	NO4-A2R	0.00	0.33	0.33	2	0.36	0.33	1.13	2	–1.54	–1.05	–1.44
	44	CB(P)-3	NO4-A3R	1.18	0.25	0.93	3	0.71	0.49	1.54	3	–2.50	–1.28	–1.24
	45	CB(P)-4	NO4-A3R	1.78	0.07	1.71	1	0.89	0.54	1.96	2	–2.82	–0.04	0.52
Group average				0.94	0.15	0.89	2.20	0.69	0.48	1.58	3.10			
Holocene–	53	DA4-D1R1	CB(P)-3	0.43	1.43	1.86	4	1.38	0.92	3.24	5	–4.77	–2.45	–2.49
Pleistocene	54	DA4-D1R2	CB(P)-3	0.42	0.83	1.25	3	1.30	0.74	2.77	2	–3.47	–1.92	–1.07
(n=12)	55	DA4-D3R1	CB(P)-3	0.25	1.24	0.99	4	0.71	0.48	1.76	0	–2.07	–3.34	–0.43
	56	DA4-D3R2	CB(P)-3	0.14	1.25	1.11	4	0.98	0.60	2.10	5	–3.56	–2.39	–2.98
	57	DA4-D5R1	CB(P)-3	0.50	1.00	0.50	4	0.57	0.41	1.30	1	–1.82	–2.88	–1.04
	58	DA4-D5R2	CB(P)-3	0.36	0.60	0.24	3	0.43	0.36	1.15	2	–1.70	–1.77	–1.53
	59	DA4-D1R1	CB(P)-4	1.03	1.61	2.64	0	1.32	0.71	2.66	6	–4.82	0.12	–1.08
	60	DA4-D1R2	CB(P)-4	1.02	1.01	2.03	1	1.39	0.67	2.39	1	–3.34	–1.01	0.80
	61	DA4-D3R1	CB(P)-4	0.35	1.42	1.77	0	0.60	0.52	1.48	1	–2.31	–0.81	0.66
	62	DA4-D3R2	CB(P)-4	0.46	1.43	1.89	0	0.88	0.57	1.75	6	–3.76	0.17	–1.76
	63	DA4-D5R1	CB(P)-4	0.10	1.18	1.28	0	0.48	0.39	1.46	2	–2.21	–0.43	–0.28
	64	DA4-D5R2	CB(P)-4	0.24	0.78	1.02	1	0.46	0.25	1.01	3	–1.97	–0.62	–1.09
Group average				0.44	1.15	1.38	2.00	0.88	0.55	1.92	2.83			
DT-DP group average				0.82	0.89	0.980	2.17	1.03	0.61	2.13	3.66			
<i>Unknowns (n=13)</i>														
Holocene–	66	DA4-D3R1	DA4-D1R1	0.68	0.19	0.87	0	0.84	0.76	2.66	5	–3.67	1.17	–1.91
Holocene	67	DA4-D3R2	DA4-D1R1	0.57	0.18	0.75	0	1.06	0.94	2.63	0	–2.73	0.24	0.46
(n=12)	68	DA4-D5R1	DA4-D1R1	0.93	0.43	1.36	0	1.20	0.67	2.70	4	–3.79	0.76	–0.96
	69	DA4-D5R2	DA4-D1R1	0.79	0.83	1.62	1	1.14	0.82	3.13	3	–3.97	–0.37	–0.66
	70	DA4-D3R1	DA4-D1R2	0.67	0.41	0.26	1	1.76	1.02	3.75	2	–4.16	0.08	–1.12
	71	DA4-D3R2	DA4-D1R2	0.56	0.42	0.14	1	1.50	1.38	4.12	7	–5.47	1.12	–3.83
	72	DA4-D5R1	DA4-D1R2	0.92	0.17	0.75	1	1.81	0.83	2.93	3	–3.93	0.25	–1.14
	73	DA4-D5R2	DA4-D1R2	0.78	0.23	1.01	2	1.63	0.96	3.22	4	–4.31	–0.30	–1.86
	75	DA4-D5R1	DA4-D3R1	0.10	0.24	0.49	0	0.53	0.51	1.87	1	–1.93	0.21	–0.35
	76	DA4-D5R2	DA4-D3R1	0.24	0.64	0.75	1	0.51	0.33	1.42	2	–1.96	–0.61	–0.80
	77	DA4-D5R1	DA4-D3R2	0.36	0.25	0.61	0	0.86	0.63	1.97	4	–2.94	0.83	–1.66
	78	DA4-D5R2	DA4-D3R2	0.22	0.65	0.87	1	0.81	0.55	1.80	3	–2.68	–0.39	–1.30
Group average				0.57	0.39	0.79	0.67	1.14	0.78	2.68	3.17			
Pleistocene–	52	CB(P)-3	CB(P)-4	0.60	0.18	0.78	4	0.37	0.26	0.95	1	–1.31	–2.46	–0.85
Pleistocene														
(n=1)														

The comparison # refers to points on Fig. 7.



- (b) Modern–Holocene. Thirty comparisons of live-collected shells with one of the six annual profiles from the three Campo don Abel shells.
- (c) Modern–Pleistocene. Ten comparisons of live-collected shells with one of the two ~ 125-ka Pleistocene Bahia la Choya shells.
- (d) Holocene–Pleistocene. Twelve comparisons of one the six annual profiles from the three Campo don Abel shells with one of the two Pleistocene Bahia la Choya shells.

In addition, several comparisons are made between shells with either unknown temporal relationships or between shells in which both the temporal and spatial relationships are unknown (Table 2):

*Holocene–Holocene.* Twelve comparisons are possible among the years sampled from the shells collected in life-position from the Campo don Abel locality. These shells have not undergone any spatial mixing. Note that these comparisons do not include comparisons of successive years from with the same shell. Such comparisons fall within the DT/SP category.

*Pleistocene–Pleistocene.* One comparison fits this category: the two shells collected from the Pleistocene deposits at Bahia la Choya. These shells were not in life position, so we know neither their exact temporal nor spatial relationships.

We radiocarbon-dated two shells from the Campo don Abel locality. Analyses were performed at the NSF-Arizona Accelerator Mass Spectrometry Laboratory at the University of Arizona. Uncalibrated 14-C dates were corrected using reservoir ages from Goodfriend and Flessa (1997).

Shell preparation and stable isotope sampling procedures were identical for all specimens. Live-collected clams were sacrificed immediately after collection and the flesh was removed. In the lab, we sectioned one valve from each specimen along the dorso-ventral axis of maximum shell height and thick sections were mounted to microscope slides. Specimens were sampled from their second, third or fourth years of growth. Sampling these early years of growth ensures that any ontogenetic decrease in growth rates does not significantly affect the annual isotopic profile (see Goodwin et al., 2003). We used 0.3 and 0.5

mm drill bits to obtain ~ 50–100 µg samples from the prismatic layer of the shell. Analyses of split samples—one half roasted and the other half unroasted—revealed no significant difference in  $\delta^{18}\text{O}$  values. Therefore, the majority of isotope samples used in this study were not roasted. Carbonate isotopic analyses were performed either on a Finnigan MAT 252 mass spectrometer equipped with Kiel III automated carbonate sampling device (University of Arizona) or on a Micromass Optima IRMS with an Isocarb common acid-bath automated carbonate device (University of California, Davis). Samples were reacted with >100% orthophosphoric acid at 70 °C (UA) or 90 °C (Davis). Samples in both labs were normalized using NBS-18 and NBS-19. Repeated measurement of carbonate standards resulted in standard deviations ( $1\sigma$ ) of  $\pm 0.08\text{‰}$ . Results are presented in permil notation with respect to the V-PDB carbonate standard.

We used periodic growth increments in the shell to fit real time to the annual isotope profiles. Because growth increments in *Chione* are deposited in response to tidal rhythms (Berry and Barker, 1975), these increments provide an independent measure of time. This approach allows comparison between different profiles regardless of growth rate, thus eliminating the limitations imposed by using sample number or sample distance on the X-axis. Shell deposition in *C. cortezi* begins in March and halts in December (Goodwin et al., 2001; Schöne et al., 2002). We assume that the timing of shell growth in *C. californiensis* is similar to *C. cortezi*. The interval between the late fall and early spring is marked in the shell by a winter band (Goodwin et al., 2001). Between winter bands, *Chione* deposits daily growth increments whose widths vary in response to the fortnightly tidal cycle (Berry and Barker, 1975; Schöne et al., 2002). Approximately 20 tidal fortnightly cycles occur between the initiation of shell deposition in the spring and the cessation of growth in the fall.

To identify fortnights, polished thick sections were examined using reflected light microscopy. Because increment widths vary with the fortnightly tidal cycle, the beginning and end of each fortnight (14 or 15 daily increments) is marked by narrow daily increments. These periodic narrow increments allowed us to identify and count fortnights and to assign  $\delta^{18}\text{O}$  samples to one of the 20 fortnights in the growth period. Because

of local environmental variations, differences in growth rates and operator error, we can assign  $\delta^{18}\text{O}$  samples to fortnights with an uncertainty of  $\pm 1$  fortnight (Goodwin et al., 2001).

Comparisons between shells are based on annual isotope profiles with  $\delta^{18}\text{O}$  values assigned to each of the 20 fortnights. However, because we did not sample every fortnight in the growth interval from individual shells, we linearly interpolated between actual  $\delta^{18}\text{O}$  values and assigned interpolated values to fortnights lacking samples. If either the first or twentieth fortnight was not sampled, the closest value was shifted to that fortnight and, if necessary, the interpolation procedure described above was performed for the intermediate fortnights. More than 20 fortnights were present in a few shells. In these shells, we trimmed alternately, the last and then the first fortnight until 20 fortnights remained. If the new first or twentieth fortnight did not have a  $\delta^{18}\text{O}$  sample, we shifted the closest  $\delta^{18}\text{O}$  value to that fortnight (even if the closest value was in a previously trimmed fortnight). If two  $\delta^{18}\text{O}$  samples were equally close to the new first or last fortnight, then the trimmed value was used. This procedure may have produced  $\delta^{18}\text{O}$  values that differ from actual values; however, without *a priori* information about

the  $\delta^{18}\text{O}$  values in unsampled fortnights, we feel our procedure is reasonable.

We devised eight metrics to compare the resulting annual isotope profiles. Each metric describes the degree of dissimilarity between a specific characteristic of two annual isotope profiles. We used principal components analysis (Octave 2.0.16; <http://www.octave.org>) on the correlation matrix of the metric scores in order to interpret the patterns of variation.

### 3. Metrics

Each of the eight metrics is based on differences in  $\delta^{18}\text{O}$  values assigned to specific fortnights during the annual growth interval. In all the metrics discussed below, larger values indicate a greater *dissimilarity*.

To illustrate these metrics, consider two hypothetical annual isotopic profiles (Fig. 3, Table 3). The metrics are as follows.

(1) Difference in maximum isotopic values ( $D_{\max}$ ): The  $D_{\max}$  is the absolute value of the difference between the maximum  $\delta^{18}\text{O}$  values from two annual isotopic profiles. The  $D_{\max}$  for the comparison between shells A and B (Fig. 3) is 0.6‰ (Table 3).

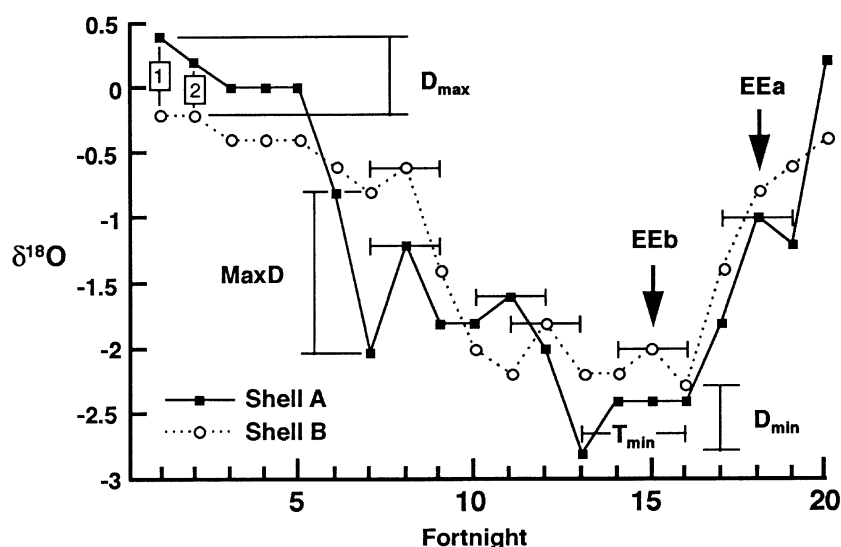


Fig. 3. Two hypothetical annual isotope profiles illustrating the eight metrics used in this study. The  $\delta^{18}\text{O}$  values as well as metric scores from the profile comparison are shown in Table 3. See text for details.



Table 3  
Fortnightly  $\delta^{18}\text{O}$  values for the hypothetical profiles shown in Fig. 3

Fortnight	Shell A	Shell B	Metric scores
1	0.4	−0.2	
2	0.2	−0.2	
3	0	−0.4	
4	0	−0.4	$D_{\text{max}}$ : 0.60
5	0	−0.4	$D_{\text{min}}$ : 0.50
6	−0.8	−0.6	$D_{\text{amp}}$ : 1.10
7	−2.0	−0.8	NNEE: 2
8	−1.2	−0.6	AD: 0.44
9	−1.8	−1.4	SDD: 0.25
10	−1.8	−2.0	MaxD: 1.20
11	−1.6	−2.2	$T_{\text{min}}$ : 3
12	−2.0	−1.8	
13	−2.8	−2.2	
14	−2.4	−2.2	
15	−2.4	−2.0	
16	−2.4	−2.3	
17	−1.8	−1.4	
18	−1.0	−0.8	
19	−1.2	−0.6	
20	0.2	−0.4	

(2) Difference in minimum isotopic values ( $D_{\text{min}}$ ): The  $D_{\text{min}}$  reports the absolute value of the difference between the minimum  $\delta^{18}\text{O}$  values. The  $D_{\text{min}}$  between shells A and B (Fig. 3) is 0.5 ‰ (Table 3).

$D_{\text{max}}$  and  $D_{\text{min}}$  record differences in the most positive and most negative  $\delta^{18}\text{O}$  values from two shells. In principle, shells that grew at the same time and in the same place will have identical maximum and minimum  $\delta^{18}\text{O}$  values. Thus,  $D_{\text{max}}$  and/or  $D_{\text{min}}$  values greater than zero may indicate that the shells did not live at the same time and/or same place.

(3) Difference in annual isotopic amplitude ( $D_{\text{amp}}$ ): The  $D_{\text{amp}}$  is simply the difference in the amplitude of annual isotopic variation in two shells. The annual isotopic amplitude of shells A and B are 3.2 ‰ and 2.1 ‰, respectively (Table 3). Thus, the  $D_{\text{amp}}$  for these hypothetical shells is 1.1 ‰.

Bivalves that lived at the same place and time should have identical annual isotopic amplitudes because each would have experienced the same seasonal range of temperature and salinity. Thus, bivalves living at the same time and place will have  $D_{\text{amp}}$  values of zero. However, shells with identical amplitudes ( $D_{\text{amp}}=0$ ) could have been alive at different places and times because two shells could have identical amplitudes but different maximum

and minimum values. Thus, the  $D_{\text{amp}}$  metric is best used in conjunction with  $D_{\text{max}}$  and  $D_{\text{min}}$  values. If bivalves grew at the same time and place, then in addition to identical annual isotopic amplitudes ( $D_{\text{amp}}=0$ ), the bivalves should have identical maximum and minimum  $\delta^{18}\text{O}$  values ( $D_{\text{max}}=0$  and  $D_{\text{min}}=0$ ).

(4) Number of non-contemporaneous enrichment events (NNEE): NNEE is the number of isotopic enrichment events from two shells that occurred at different times during the growth interval. An enrichment event (EE) is a local positive  $\delta^{18}\text{O}$  anomaly and is defined as a set of three  $\delta^{18}\text{O}$  samples where the first is followed by a second with a more positive value, which is in turn followed by a sample with a more negative value. Enrichment events result from either temporary cooling and/or evaporative enrichment of the water in which the clams grew. In the example presented in Fig. 3, both shells have three enrichment events. In shell A, EEs occur in fortnights 8, 11 and 18; in shell B, EEs occur in fortnights 8, 12 and 15. EEs that occur in the same fortnight in different shells are contemporaneous; EEs that occur in different fortnights are non-contemporaneous. However, because  $\delta^{18}\text{O}$  samples are assigned to fortnights with an error of  $\pm 1$  fortnight, samples whose error bars overlap are considered here as contemporaneous. The first enrichment event in both shells occurs in fortnight 8 and thus the two events are contemporaneous. The second EE in shell A occurs in fortnight 11 and fortnight 12 in shell B. Because the error bars from the fortnight assignments overlap (see Fig. 3), the possibility that these enrichment events occurred at the same time cannot be ruled out. Thus, these two enrichments are considered contemporaneous. The third EE in shells A and B occurs in fortnight 18 and 15, respectively. Because the error bars of these samples do not overlap, these enrichment events occurred at different times (Fig. 3, EEa and EEb). Thus, the NNEE metric for the comparison of shells A and B is two (one in each shell).

Bivalves alive in the same location will experience and record isotopic perturbations at the same time. Thus, the number of non-synchronous enrichment events in shells living at the same time in the same place should be zero. NNEEs greater than zero indicate that the specimens being compared were not living at the same time and/or same place.

The next three metrics compare  $\delta^{18}\text{O}$  values from corresponding fortnights: the  $\delta^{18}\text{O}$  value from the first fortnight in one shell is compared to the  $\delta^{18}\text{O}$  value from the first fortnight in a second shell, etc. Because each annual growth interval consists of 20  $\delta^{18}\text{O}$  values, there are 20 comparisons for each pair of shells. The following metrics are based on 1 or all of these 20 comparisons.

(5) Average difference (AD): AD is the average of the differences from each of the 20 fortnight comparisons. The average difference between shells A and B (Fig. 3) for all 20 fortnights is 0.44‰ (Table 3).

(6) Standard deviation of the differences (SDD): SDD is the standard deviation of the 20 fortnight comparisons. In the example from Fig. 3, the SDD is 0.25‰.

(7) Maximum difference (MaxD): This metric records the maximum  $\delta^{18}\text{O}$  difference that occurs in the comparisons of the 20 fortnights. In the hypothetical example, the MaxD is 1.2‰ and occurs in fortnight seven (Fig. 3, Table 2).

Values for AD, SDD and MaxD should be small for shells alive at the same time and place; shells which lived at different times and/or different places should have larger AD, SDD and MaxD values.

(8) Timing of minimum value ( $T_{\min}$ ):  $T_{\min}$  is the number of fortnights between the minimum values in the two annual profiles. In Fig. 3, the minimum  $\delta^{18}\text{O}$  value in shell A occurs in fortnight 13 and fortnight 16 in shell B. Thus, the  $T_{\min}$  for this comparison is 3.

## 4. Results and discussion

### 4.1. Same time/same place comparison: why aren't they identical?

Because temperature and the isotopic composition of water control the fractionation of oxygen isotopes in biogenic carbonates (Grossman and Ku, 1986), proximal clams living at the same time should have identical annual  $\delta^{18}\text{O}$  profiles. IM11-A1L and IM11-A2L lived at the same time ~ 2 m apart. Goodwin et al. (2001) showed that the timing of the initiation of shell deposition in 1999 from both specimens was nearly identical (IM11-A1L: March 26, 1999; IM11-A2L: March 29, 1999). Similarly, the cessation of

growth in both specimens occurred in late November or early December. In addition, daily increment-width profiles from both specimens were similar (see Figs. 5c and 6c in Goodwin et al., 2001). These similarities suggest that the patterns of growth from the two shells are nearly identical. Are the patterns of annual  $\delta^{18}\text{O}$  variation identical?

On a scatter plot the  $\delta^{18}\text{O}$  values from clams with identical isotope values should fall along a straight line with a slope = 1 (Fig. 4). The  $\delta^{18}\text{O}$  values from the contemporaneous adjacent clams are highly correlated (correlation coefficient = 0.89). The overall similarity of the observed data to the expected values suggests that  $\delta^{18}\text{O}$  profiles can be used as a standard with which to evaluate temporal and spatial mixing.

Note, however, that the fit is not perfect. The deviation from a perfect fit likely reflects three factors:

1. Biological. Small differences in the response of individual clams to temperature, salinity and nutrient availability can result in sclerochronological and isotopic variation. Thus, like snowflakes, no two clams are exactly alike.
2. Methodological. Clams grow at different rates throughout the year, making it difficult to accurately establish the timing of deposition of sub-annual growth increments (Goodwin et al., 2001).

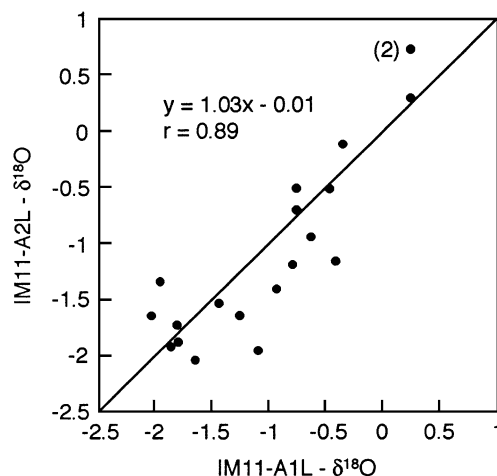


Fig. 4. Plot of sclerochronologically calibrated  $\delta^{18}\text{O}$  values from two clams living at the same time in the same place (IM11-A1L and IM11-A2L). See text for discussion.

This is especially true for the narrow growth increments deposited at or near the upper and lower temperature thresholds of growth. Thus,  $\delta^{18}\text{O}$  samples are assigned to fortnights with an error of  $\pm 1$  fortnight. Some of the lack of fit likely reflects imprecise assignment to fortnights. Because the  $\delta^{18}\text{O}$  value likely varies slightly throughout a fortnight, the position of the sample within a fortnight may also contribute to the difference. Another methodological error is a result of sampling density. Because not all fortnights within the growth interval were sampled, some  $\delta^{18}\text{O}$  values are interpolations that may not reflect actual environmental conditions. The magnitude of this error becomes greater with increasing distance between actual  $\delta^{18}\text{O}$  samples.

3. Analytical. Each oxygen-isotope value is affected by instrument error. All isotopic measurements are associated with a certain degree of uncertainty, here  $\pm 0.08\%$ . Thus, even if the first two sources of error discussed above could be eliminated, a certain level of uncertainty is inevitable.

Although the correlation between the  $\delta^{18}\text{O}$  variation in IM11-A1L and IM11-A2L is high, the scatter plot (Fig. 4) cannot reveal the causes of the differences in the isotope profiles. However, the eight metrics reflect specific differences between annual profiles, and can be used to identify the causes of isotopic variation among clams with various spatial and temporal relationships.

#### 4.2. Individual metrics

##### 4.2.1. Using the metrics: a univariate approach

Seventy-eight comparisons, of eight metrics each, were generated from the 13 annual isotope profiles (Table 2). The average number of samples per year is 12.7; the maximum is 22 (NO4-A2R) and the minimum is 7 (DA4-D1R). Actual and interpolated  $\delta^{18}\text{O}$  values are shown in the appendix, the 13 annual isotope profiles are shown in Fig. 5. Variation of the values for each metric provides insight into the sensitivity of the metrics as indicators of temporal and spatial mixing (Fig. 6 and Table 2).

In principle, the single comparison of shells alive at the same time in the same place should yield values of

zero for all eight metrics. That it does not (with the exception of NNEE), undoubtedly reflects the biotic, methodological and analytical errors discussed above. Nevertheless, this comparison can serve as the standard by which temporal and spatial mixing can be detected. Values consistently higher than the ST/SP comparisons suggest either time-averaging, spatial mixing or both.

Inspection of the individual metrics shows that with but three exceptions, the range of variation among DT/DP comparisons encompasses all of the other comparisons (Fig. 6, Table 2). The first exception is the AD (Fig. 6E), in which the ST/SP comparison falls below the range of the DT/DP comparisons. Another exception is the SDD (Fig. 6F); here too the single ST/SP comparison falls below the range of the different DT/DP comparisons. The third exception is the MaxD metric (Fig. 6G); here the ST/SP and the Pleistocene–Pleistocene comparisons fall below the DT/DP comparisons. In these exceptions, the ST/SP and Pleistocene–Pleistocene metric values are only slightly below the range of the DT/DP comparisons. This suggests that in univariate space, at least, there is little obvious separation of values into the four different spatial and temporal categories.

Nevertheless, some significant patterns are evident. The  $D_{\min}$  metric measures the difference in minimum isotopic values. In environmental settings in which there is little variation in the isotopic composition of the ambient seawater, the maximum temperature experienced during growth largely controls the minimum  $\delta^{18}\text{O}$  value; recall that low  $\delta^{18}\text{O}$  values result from high temperatures. However, if significant amounts of isotopically negative river water are mixed with the ambient seawater,  $D_{\min}$  values from comparisons of shells grown in the absence of river water with shells grown in brackish water will be higher than in comparisons of shells grown only in the absence of river water. Note, for example, that the Modern–Modern  $D_{\min}$  values among the DT/DP comparisons are at the low end of the distribution (Fig. 6B). All these shells grew without any influence of Colorado River water. In contrast, comparisons of Modern and Holocene shells show much higher  $D_{\min}$  values, a reflection of the effect of river water on isotopic variation in the Holocene.

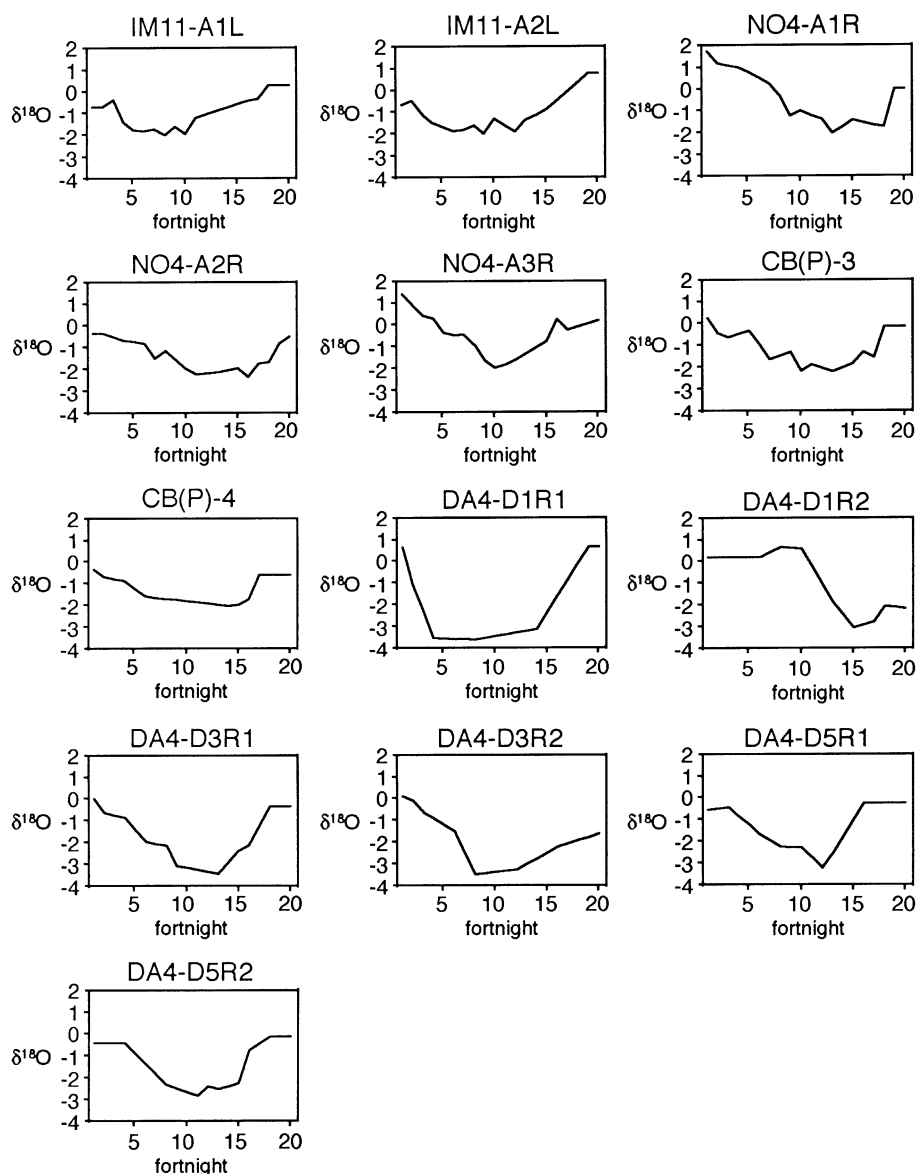


Fig. 5. Thirteen observed annual isotope profiles from the 10 shells used in this study. Each profile consists of 20 observed or interpolated  $\delta^{18}\text{O}$  values. Isotope data are shown in Appendix A.

The same contrast is provided by the differences in  $D_{\min}$  values in the Modern–Pleistocene comparisons and those in the Holocene–Pleistocene comparisons. Neither of the shells from the Pleistocene deposit shows isotopic values indicative of river water influx. Thus, the Modern–Pleistocene  $D_{\min}$  values are more similar to those of the Modern–

Modern comparisons and the Holocene–Pleistocene values are more similar to those of the Modern–Holocene comparisons.

The lack of a freshwater effect in the isotopic composition of the Pleistocene shells does not mean that the Colorado River did not flow into the Gulf at this time. The Bahia la Choya Pleistocene locality was

too far from the mouth of the river to show the effects. Before upstream river diversions, the mixing zone of river and seawater extended only about 65 km from the river's mouth (Rodriguez et al., 2001). Today, the Bahia la Choya locality is  $\sim 110$  km distant from the mouth of the river. Furthermore, because of delta progradation the river's mouth was probably farther north during the last interglacial,  $\sim 125$  ka ago.

The low  $D_{\min}$  values in the Modern–Pleistocene comparisons, and their similarity to the  $D_{\min}$  values of the Modern–Modern comparisons, suggests that there is just as much variation in  $D_{\min}$  between shells that are only a few years apart as there is between shells that differ in age by  $\sim 125$  ka. But temporal differences, per se, do not cause isotopic differences; environmental differences cause isotopic differences. If summer temperatures during the last interglacial were similar to summer temperatures today, then differences in minimum  $\delta^{18}\text{O}$  values ( $D_{\min}$ ) will differ only by the difference in the isotopic composition of the seawater.

The isotopic composition of seawater during the last interglacial was slightly more negative than today because smaller ice caps stored a smaller amount of  $^{16}\text{O}$ . Chappell and Shackleton (1986) suggested that sea level during the last interglacial was  $\sim 6$  m higher than today. Assuming 0.01 ‰ for each meter of sea-level difference (Shackleton, 1986), this would result in last-interglacial ocean water 0.06 ‰ more negative than today. This shift is small relative to the intra-annual  $\delta^{18}\text{O}$  amplitudes for modern *Chione*. We did not adjust the values of the Pleistocene shells to reflect this difference.

If the influx of river water affects  $D_{\min}$  values, why doesn't it affect  $D_{\max}$  (Fig. 6A) values? Before upstream river management, the Colorado's flow was strongly seasonal. Approximately 70% of the river's annual flow arrived at the delta in only 3 months: May, June and July (Harding et al., 1995). This large pulse of isotopically negative freshwater marked the arrival of the annual spring snowmelt and coincided with some of the hottest months of the year. However, the maximum  $\delta^{18}\text{O}$  values are recorded in the shell shortly before the fall cessation of growth and just after the spring initiation, when river flow (and the influx of isotopically negative river water) was at a minimum. Thus, maximum values are less likely to be reduced by the effects of river water than minimum values.

Consider now the ranking among the eight metrics, among the four known temporal/spatial categories. In Table 4, the temporal/spatial category with the lowest average metric score was assigned the lowest rank (1); the category with the highest average metric score was assigned the highest rank (4). The ST/SP category has the lowest rank in five of the eight metrics and the DT/DP category ranks highest in four out of the eight metrics. The DT/SP and ST/DP categories often occupy intermediate ranks. Summing the ranks makes the picture clearer. As might be expected, the pair in the ST/SP category ranks lowest, the average of the DT/SP comparisons is next, then the comparison from the ST/DP, and finally the DT/DP group average is the highest. That the DT/DP comparisons rank highest is predictable. After all, year-to-year environmental differences plus place-to-place environmental differences maximizes the chances that isotopic variation will differ in any pair of shells from different times and different places.

Does variation from year-to-year cause more dissimilarity than variation from place-to-place? Here, because of small sample sizes, we can only speculate, but note that the lower ranking of the DT/SP group relative to the ST/DP pair suggests that year-to-year environmental variation might cause less isotopic variation than place-to-place environmental variation. The relative ranking of the two intermediate categories persists, even after eliminating the comparisons of successive years in the Holocene shells (see Table 2). Although this is not a statistically rigorous argument, it does make sense. If the annual  $\delta^{18}\text{O}$  variation is driven largely by temperature, evaporation and the influx of river water, shells living in the same place but at different times will likely experience similar seasonal temperature extremes and similar evaporative regimes. Year-to-year variation in river discharge will cause some isotopic differences. But shells living at the same time, but in different places—either in different positions with respect to the tide, or in substantially different locations—may experience significant different temperatures and evaporative regimes, in addition to different proportions of river water and seawater.

#### 4.2.2. Using the metrics: shells with unknown relationships

Although the spatial relationships of the Holocene shells are known because they occurred in life position

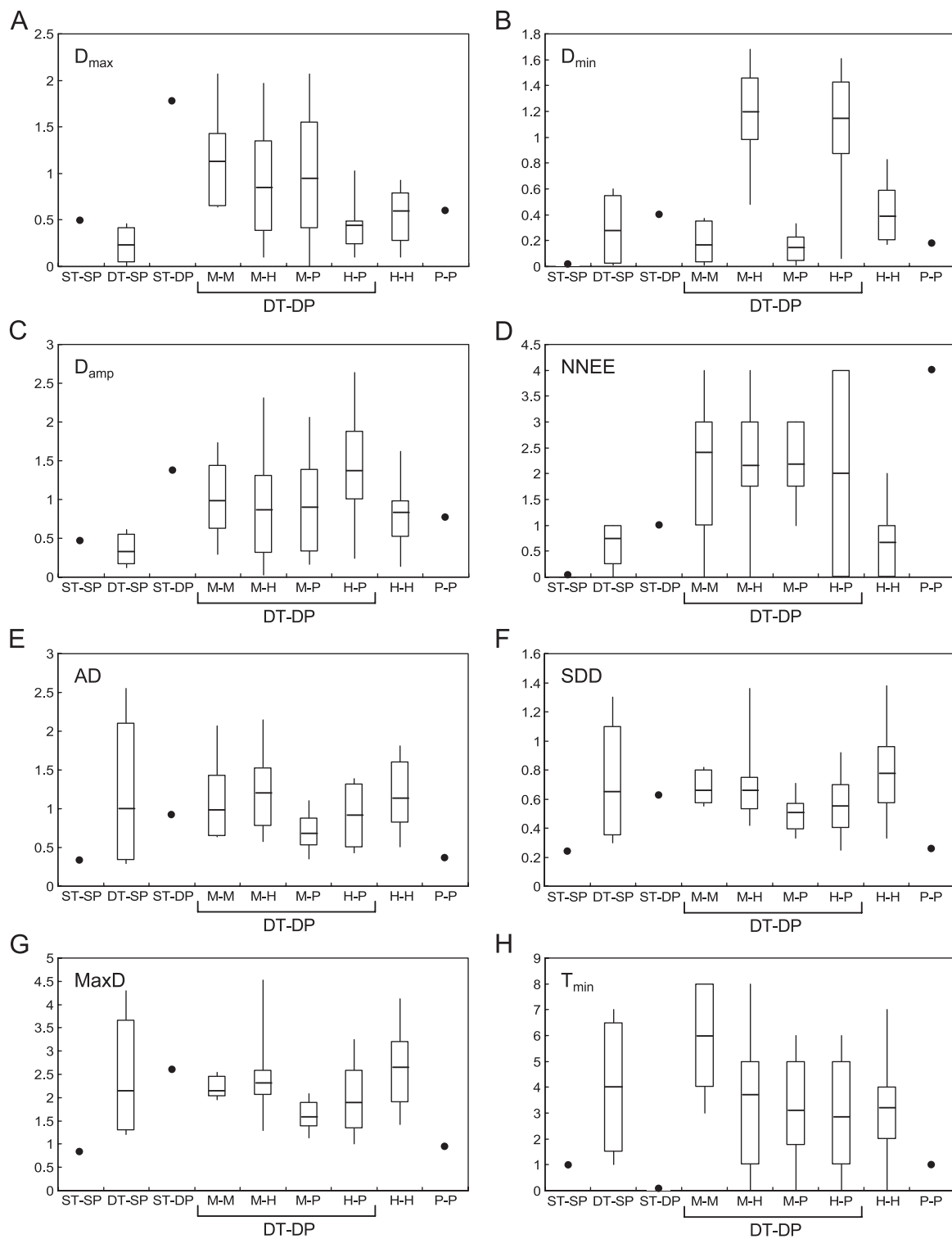




Table 4

Relative ranks of the four temporal/spatial categories for each metric

Temporal/spatial category	$D_{\max}$	$D_{\min}$	$D_{\text{amp}}$	NNEE	AD	SDD	MaxD	$T_{\min}$	Sum of ranks
Same time/same place	2	1	2	1	1	1	2	1	11
Different time/same place	1	2	1	2	3	3	3	4	19
Same time/different place	4	3	4	3	4	2	1	3	24
Different time/different place	3	4	3	4	2	4	4	2	26

See text for discussion.

within a meter of each other, their exact temporal relationships are not known. Uncorrected radiocarbon ages of two shells from the Holocene deposit at Campo don Abel are indistinguishable:  $1370 \pm 55$  and  $1360 \pm 48$  ybp (Table 1). Calibrated  $2\sigma$  age ranges from the online CALIB radiocarbon calibration program (<http://depts.washington.edu/qil/calib>) are 530–354 and 519–352 ybp (Table 1). Radiocarbon dating places the shells within  $\sim 100$  years of each other, but that number is simply the resolution of the dating technique. Time-averaging of less than 100 years could have taken place. If we use the ST/SP pair as the standard for no temporal mixing, the eight metrics of the standard pair are less than any pair-wise comparison of the Holocene shells in four ( $D_{\min}$ , AD, SDD, MaxD) of the eight metrics (Table 2, Fig. 6A–H). In the remaining metrics,  $D_{\max}$  in the standard is less than in 8 of the 12 pair-wise comparisons,  $D_{\text{amp}}$  is less than in 10 comparisons, NNEE is less than in 7 pairs and  $T_{\min}$  is less than in 10 comparisons (Table 2). No single pair of shells in the Holocene group scores consistently low for all metrics; the low values are scattered among all the comparisons. We conclude that none of the years sampled in the Holocene shells are the same. The deposit is time-averaged.

The two Pleistocene shells provide only a single comparison (Table 2). These shells were not in life position and were disarticulated. Neither their temporal nor their spatial relationships are known. Pleistocene–Pleistocene values are greater than the ST/SP pair in all metrics except  $T_{\min}$ , where it is the same. In

four of the metrics, the values are similar, differing by less than 25% in  $D_{\max}$ , AD, SDD and MaxD. By comparison with the Holocene assemblage, the Pleistocene–Pleistocene values are lower in four metrics (AD, SDD, MaxD,  $T_{\min}$ ), are indistinguishable in three ( $D_{\max}$ ,  $D_{\min}$ ,  $D_{\text{amp}}$ ) and exceed them in one (NNEE). With the exception of MaxD, all the Pleistocene–Pleistocene values fall within the range of the DT/DP comparisons. The very high NNEE value of the Pleistocene–Pleistocene comparison is striking. It seems unlikely that four non-contemporaneous enrichment events could have occurred in contemporaneous and adjacent shells. Indeed, five enrichment events occur in one shell (CB(P)-3), only one of which occurs in the other (CB(P)-4). We suspect that the shell with the five enrichment events was living in the upper part of the intertidal zone, where evaporative enrichment of tide pool water occurred during neap tides. We conclude that the two Pleistocene shells are both temporally and spatially mixed. The similarity of the values to those of the Holocene comparisons suggests time-averaging of a similar magnitude, and the number of non-contemporaneous enrichment events suggests spatial mixing across the intertidal zone—a distance of 1–2 km.

#### 4.3. Multivariate analysis

##### 4.3.1. Principal components analysis

Principal components analysis reveals the patterns of correlation among the eight metrics. The analysis is

Fig. 6. Box plots showing the variation of metrics in each temporal and spatial category and in the unknown comparisons. Single values are shown by dashes. Average values shown by horizontal line within box; upper 75% value defines top of box; lower 25% defines bottom of box; range shown by vertical line. ST-SP ( $n=1$ ): same time/same place; DT-SP ( $n=4$ ): different time/same place; ST-DP ( $n=1$ ): same time/different place. The different time/different place (DT-DP,  $n=59$ ) category has been divided into four subgroups: Modern–Modern comparisons (M–M,  $n=7$ ), Modern–Holocene (M–H,  $n=30$ ), Modern–Pleistocene (M–P,  $n=10$ ) and Holocene–Pleistocene (H–P,  $n=12$ ). Two categories have unknown temporal/spatial affinities. The Holocene–Holocene comparisons (H–H,  $n=12$ ) are from shells collected articulated and in life-position. The Pleistocene–Pleistocene comparison (P–P,  $n=1$ ) is based on two disarticulated shells with unknown temporal and spatial affinities.

based on the correlation matrix of the 78 comparisons plus a comparison of 2 identical annual profiles with a score of 0 for each metric. Each of the eight metrics strongly loads on only one of the first three principal component axes (PCs), which together explain ~ 70% of the variation (Table 5). Therefore, only the first three axes will be discussed.

The AD, SDD and MaxD load highly on the first principal component, which explains 40% of the variation of the comparisons (Table 5). These three metrics have low values when the profiles being compared have similar shapes. The shape of individual profiles is principally controlled by seasonal temperature changes. We interpret the first principal component as reflecting the basic concave shape—and by extension the seasonal temperature variation—of the annual isotope profiles (Fig. 4).

The difference in minimum value ( $D_{\min}$ ) and the NNEE load highly on the second principal component, which explains 14% of the variation in the differences between profiles (Table 5). Both metrics are especially sensitive to changes in hydrologic regime, either by evaporation or addition of isotopically light river water. Therefore, the second principal component reflects variation in the isotopic composition of the water in which the clams grew.

Three metrics have high loadings on the third principal component (Table 5): The difference in maximum value ( $D_{\max}$ ), the difference in amplitude ( $D_{\text{amp}}$ ) and the difference in the timing of the minimum value ( $T_{\min}$ ). The third principal component explains 14% of the overall variation in the differences between the profiles. These metrics are sensitive

Table 5

Factor loadings for each metric in the first three principal component axes

	PC1	PC2	PC3
$D_{\max}$	-0.148	0.230	0.574
$D_{\min}$	-0.245	-0.630	0.086
$D_{\text{amp}}$	-0.174	-0.233	0.570
NNEE	0.005	-0.570	-0.261
AD	-0.540	0.112	-0.082
SDD	-0.527	-0.015	-0.110
MaxD	-0.520	0.112	-0.090
$T_{\min}$	-0.218	0.191	-0.503
% variation explained	39.7	14.4	14.2

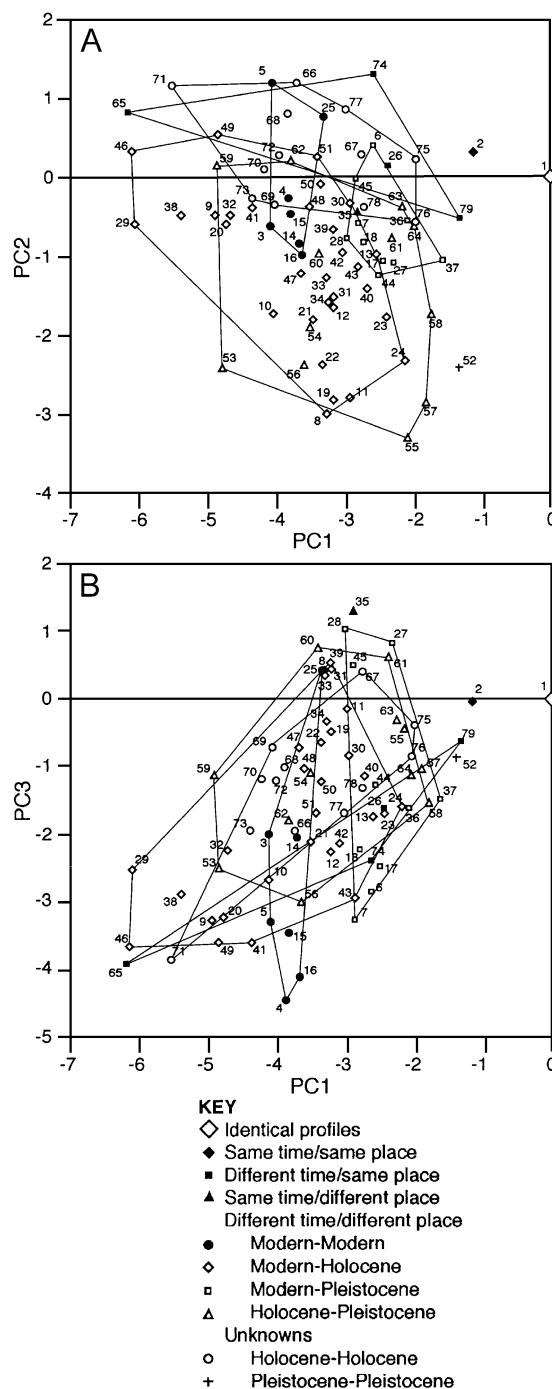


Fig. 7. Distribution of the 78 actual profile comparisons as well as the identical profile comparison in multivariate space. (A) Principal component 1 versus principal component 2; (B) principal component 1 versus principal component 3. Lines surround points from each temporal/spatial category (see Table 2). See text for discussion.

to the magnitude and timing of changes in the isotopic composition and temperature of the water.

Individual comparisons are plotted in principal component space in Fig. 7. For reference, the position of the comparison of two hypothetical identical isotopic profiles is shown at the intersection of the principal components.

The single comparison of shells from the same time and same place (#2) does not plot in the same position as the comparison of the identical profiles, but it is the closest comparison to that point (Fig. 7A). As discussed above in the context of the regression of the  $\delta^{18}\text{O}$  values from the adjacent shells and the various individual metrics, the ST/SP shells depart from perfect identity because of some combination of biological, methodological and analytical differences. None of the other comparisons fall within the radius defined by the distance from #2 to the comparison of identical profiles, suggesting that shells that differ in time or space will be a greater distance from the intersection of the principal component axes than the two adjacent shells compared here.

DT/SP comparisons vary mostly along PC1; this variation is largely determined by the position of #65, a comparison of successive years in the same shell. The comparison of these 2 years yields high values of AD, SDD and MaxD. The remaining three shells in the DT/SP group vary mostly along PC2 and PC3, axes reflecting differences in the timing and magnitude of differences in isotopic composition and maximum temperature.

The single comparison of shells from the ST/DP (#35) is within the overall cloud of points on the PC1 vs. PC2 graph (Fig. 7A), but is the highest scoring point on PC3 (Fig. 7B). This comparison has some of the greatest differences in  $D_{\text{max}}$  and  $D_{\text{amp}}$  combined with the smallest difference in  $T_{\text{min}}$  (Table 2).

Among the comparisons of shells from different times and different places, the Modern shells vary little along PC1 or PC2, but greatly along PC3, indicating differences among the shells in  $D_{\text{max}}$ ,  $D_{\text{amp}}$  and  $T_{\text{min}}$ . Comparisons of Modern shells with those in the Holocene group vary along all three principal components, reflecting isotopic differences between times of river flow and times of no river flow, as well as differences caused by temporal and spatial environmental variation. In contrast, there is less variation among comparisons of Modern shells and those from

the Pleistocene deposit. These comparisons are relatively closer to the intersection of the three principal components than are the comparisons between the Modern and Holocene shells. Indeed, they are closer than the comparisons among just the Modern shells. This suggests that differences between similar climatic regimes—the present and the previous interglacial—are no greater than differences that occur within the present climatic regime.

After all, temporal variation does not cause the environmental variation that results in isotopic differences. Because climate change is often cyclical, the same conditions can recur many times during a long time interval. Shells differing in age by 125,000 years are more similar to each other because of a similar climatic regime than are shells that differ only by  $\sim 500$  years, but experienced the isotopic effects of varying Colorado River influx. Thus, temporal variation is an imperfect proxy for environmental variation. Only in instances of monotonic environmental change could isotopic differences increase with increasing temporal differences.

Comparisons of Holocene and Pleistocene shells vary in a fashion similar to the Modern–Holocene comparisons. This is largely a consequence of the similarity of the Pleistocene shells to the Modern shells. Both are from a similar climatic regime and each is being compared to shells alive during the input of isotopically negative river water.

#### 4.3.2. Multivariate analysis and the unknowns

The Holocene shells are all from the same place, but their exact temporal affinities are unknown. Two comparisons (#75 and #76) plot close to the pair known to have lived at the same time and place, while others (#71 and #73) are as distant as shells from drastically differing regimes of Colorado River flow (Fig. 7A and B). The same pair of shells is involved in comparisons 75 and 76 (Table 2): 2 successive years of DA4-D5R and the first year of DA4-D3R. These two individuals may have been near-contemporaries, whereas DA4-D1R (in comparisons #71 and #73) appears to have been alive at a different time.

This conclusion is supported by  $\delta^{18}\text{O}$  values from the commissures of the shells. If the clams died at the same time the  $\delta^{18}\text{O}$  values at the commissures should be identical (Shackleton, 1973). However, this is not the case. In fact, each shell from Campo don Abel has a

different commissure value (DA4-D1R,  $-3.92\text{‰}$ ; DA4-D3R,  $-2.63\text{‰}$ ; DA4-D5R,  $-0.91\text{‰}$ ). These values indicate that the clams died at different times, further supporting the conclusion that they were not contemporaries.

The single comparison of the Pleistocene shells is distant from the intersection PC1 and PC2, but lies close to the known ST/SP comparison along PC3. The low score on PC2, reflecting strong differences in NNEE suggests that the two shells were in different evaporative regimes, leading to several non-contemporaneous enrichment events. We conclude that the two Pleistocene shells were alive at different times and in different places.

## 5. On the application of the method

Two issues must be carefully considered before applying this method to deposits with unknown spatial and/or temporal relationships. First, the metrics used to make comparisons between different  $\delta^{18}\text{O}$  profiles should reflect geochemical variations observed in the region in question. For example, in the northern Gulf of California, evaporation rates are high. Combined with the extreme tidal range, this causes significant evaporative enrichment of stranded pools during neap tides. This set of local environmental conditions leads to enrichment events observed in the shells from clams living in the high-intertidal zone (see above). However, observable enrichment events may not be present in shells living in a region with lower amplitude tides or less-extreme evaporative regimes. The number of non-contemporaneous enrichment events would be an ineffective metric when comparing shells from such a region and should not be included. Nevertheless, certain metrics, such as  $D_{\text{max}}$ ,  $D_{\text{min}}$ ,  $D_{\text{amp}}$ , AD, SDD and MaxD, should be universally applicable.

Second, the distribution of metric values from shells with known spatial and temporal relationships must be defined. This variability can then be used to evaluate comparisons with unknown spatial/temporal relationships. That is, when several shells from the same spatial/temporal category are compared their individual metric values are likely to be different. For example, if 5 shells alive at the same time and place are compared (yielding 10 comparisons), the 10 numbers from each metric will yield a distribution of

values. Metric values from unknown shells can then be statistically compared with this distribution. This procedure can be performed for each metric used in the analysis, yielding quantitative evaluations of temporal and/or spatial mixing. A similar strategy can be used with the principal component analysis or another multivariate technique. Here, known comparisons will be distributed over some area in multivariate space. Profile comparisons based on unknowns can then be checked to determine if they fall within the region defined by shells with known relationships. Together, site-specific metrics and analysis of the variability of the knowns, make this approach a flexible, quantitative tool for identifying temporal and spatial mixing in fossil assemblages.

## 6. Conclusions

1. Individual mollusks of the same species living at the same time and same place will have nearly identical stable oxygen isotope profiles. Differences in annual isotope profiles can indicate temporal or spatial mixing.
2. Differences in annual isotopic profiles can be measured by calculating metrics: the difference in maximum value, difference in minimum value, difference in amplitude, the number of non-synchronous enrichment events, the average fortnightly difference, the standard deviation of the average fortnightly difference, the maximum fortnightly difference and the difference in the fortnight of the minimum value.
3. These metrics vary among comparisons of shells of the Gulf of California venerid bivalves *C. cortezi* and *C. californiensis* from the same time/same place, different time/different place, same time/different place and different time/different place.
4. A pair of shells from the same time and same place has the lowest average dissimilarity, while shells from different times and different places tend to have the highest dissimilarity. Comparisons of shells from the same time/different place and different time/same place have intermediate values.
5. Multivariate analysis shows that three principal components (overall shape, differences in isotopic composition of the water and differences in the magnitude and timing of isotopic minima) explain

approximately 70% of the variation in dissimilarity. The same time/same place comparison lies closest to the origin of the principal component axes.

6. In the northern Gulf of California, unless significant variation in freshwater influx occurs through time, spatial variation is likely to cause more isotopic differences than temporal variation.
7. Both univariate and multivariate approaches suggest that adjacent, in-situ Holocene shells of unknown temporal affinities were alive at different times. In the single comparison of Pleistocene shells, in which both temporal and spatial relationships are unknown, univariate and multivariate approaches indicate that the two shells were alive at different times and in different elevations within the intertidal zone.
8. Univariate and multivariate comparisons of annual isotopic profiles can be powerful tools for evaluating temporal and spatial mixing in fossil assemblages.

## **Acknowledgements**

We thank J. Campoy, A. Garry, E. Johnson and C. Rodriguez for help in the field. H. Spero, at the University of California, Davis, performed some of the isotopic analyses. We also thank the skilled boat captains from El Golfo de Santa Clara, Sonora. Thanks also to P. Roopnarine for thoughtful discussions and advice, as well the Octave principal component script. We thank D. Jones, J. Pandolfi and an anonymous reviewer for their helpful comments on an earlier version of this manuscript. Special thanks also to W. Allmon and A. Longinelli whose careful and thoughtful reviews significantly improved this paper. This study was funded by grants from the National Science Foundation, the Eppley Foundation for Research, the Alexander-von-Humboldt Foundation (Lynen Program) and Consejo Nacional de Ciencia y Tecnología. This is CEAM publication #48.

## Appendix A

$\delta^{18}\text{O}$  values for each annual isotope profile. Values marked with “\*” are interpolated. See text for details

Fortnight	IM11-A1L	IM11-A2L	NO4-A1R	NO4-A2R	NO4-A3R	CB(P)-3	CB(P)-4	DA4-D1R1	DA4-D1R2	DA4-D3R1	DA4-D3R2	DA4-D5R1	DA4-D5R2
1	-0.77*	-0.70	1.67	-0.40*	1.38	0.20	-0.40	0.59	0.15*	-0.05	0.06	-0.59	-0.46*
2	-0.77	-0.52	1.13	-0.40	0.88*	-0.46	-0.74	-1.13	0.15*	-0.68	-0.12	-0.53*	-0.46*
3	-0.43	-1.16	1.03*	-0.57*	0.37	-0.67	-0.83	-2.36*	0.15*	-0.81*	-0.67	-0.47	-0.46*
4	-1.45	-1.53	0.93	-0.73	0.28	-0.52*	-0.93	-3.59	0.15*	-0.93	-0.96*	-0.89*	-0.46
5	-1.81	-1.73*	0.73	-0.78	-0.39	-0.37	-1.28*	-3.61*	0.15*	-1.47*	-1.25*	-1.30*	-0.93*
6	-1.86	-1.92	0.46*	-0.86	-0.50	-1.02*	-1.63	-3.64*	0.15	-2.01	-1.54	-1.72	-1.40*
7	-1.80	-1.88	0.20	-1.54	-0.49	-1.67	-1.70	-3.66*	0.39*	-2.11*	-2.52*	-2.02*	-1.86*
8	-2.05	-1.65	-0.38	-1.18	-0.95	-1.51*	-1.75*	-3.68	0.62	-2.20	-3.5	-2.31	-2.33
9	-1.65	-2.03	-1.3	-1.59*	-1.65	-1.35	-1.80*	-3.60*	0.58*	-3.11	-3.45*	-2.33*	-2.50*
10	-1.97	-1.34	-1.05	-2.00	-2.00	-2.23	-1.85*	-3.51*	0.54	-3.21*	-3.40*	-2.34	-2.68*
11	-1.26	-1.65	-1.26	-2.29	-1.88	-1.93	-1.90	-3.43*	-0.28*	-3.30*	-3.35*	-2.80*	-2.85
12	-1.10*	-1.95	-1.44	-2.24*	-1.61*	-2.09*	-1.96*	-3.34*	-1.11*	-3.40*	-3.30	-3.25	-2.43
13	-0.94*	-1.40	-2.06	-2.19	-1.34*	-2.25	-2.01*	-3.26*	-1.93	-3.49	-3.04*	-2.63	-2.54
14	-0.79*	-1.19	-1.78*	-2.09*	-1.06*	-2.06*	-2.07	-3.17	-2.51*	-2.96*	-2.79*	-1.85	-2.42*
15	-0.63*	-0.93	-1.49	-1.99	-0.79	-1.87	-2.01	-2.41*	-3.08	-2.42	-2.53*	-1.08*	-2.29
16	-0.47	-0.52*	-1.59*	-2.40	0.20	-1.34	-1.76	-1.65*	-2.95*	-2.17	-2.27	-0.30	-0.75
17	-0.36*	-0.10*	-1.70*	-1.78	-0.27	-1.60	-0.65	-0.89*	-2.81	-1.29*	-2.12*	-0.30*	-0.46*
18	0.24	0.32*	-1.80	-1.71	-0.13*	-0.19	-0.65*	-0.13*	-2.12	-0.4	-1.96*	-0.30*	-0.16
19	0.24*	0.73	-0.05	-0.85	0.02*	-0.19*	-0.65*	0.63	-2.16*	-0.40*	-1.81*	-0.30*	-0.16*
20	0.24*	0.73*	-0.05*	-0.54	0.16	-0.19*	-0.65*	0.63*	-2.20	-0.40*	-1.65	-0.30*	-0.16*



## References

- Aberhan, M., Fürsich, F.T., 1991. Paleocology and paleoenvironments of the Pleistocene deposits of Bahia la Choya (Gulf of California, Sonora, Mexico). *Zitteliana* 18, 135–164.
- Allison, P.A., Briggs, D.E.G. (Eds.), 1991. *Taphonomy, Releasing the Data Locked in the Fossil Record*. Plenum, New York.
- Behrensmeier, A.K., Kidwell, S.M., Gastaldo, R.A., 2000. Taphonomy and Paleobiology. In: Erwin, D.H., Wing, S.L. (Eds.), *Deep Time. Paleobiology's Perspective*. Paleontological Society, Lawrence, Kansas, pp. 103–147.
- Berry, W.B.N., Barker, R.M., 1975. Growth increments in fossil and modern bivalves. In: Rosenberg, G.D., Runcorn, S.K. (Eds.), *Growth Rhythms and the History of the Earth's Rotation*. Wiley, New York, pp. 9–25.
- Bianucci, G., Longinelli, A., 1982. Biological behavior and accretion rates of *Patella coerulea* L. as indicated by oxygen isotope measurements. *Palaeogeography, Palaeoclimatology, Palaeoecology* 37, 313–318.
- Cespuglio, G., Piccinetti, C., Longinelli, A., 1999. Oxygen and carbon isotope profiles from *Nassa mutabilis* shells (Gastropoda): accretion rates and biological behavior. *Marine Biology* 135, 627–634.
- Chappell, J., Shackleton, N.J., 1986. Oxygen isotopes and sea level. *Nature* 324, 137–140.
- Flessa, K.W., 1993. Time-averaging and temporal resolution in recent marine shelly faunas. In: Kidwell, S.M., Behrensmeier, A.K. (Eds.), *Taphonomic Approaches to Time Resolution in Fossil Assemblages*. Short Courses in Paleontology, vol. 6. Paleontological Society, Knoxville, pp. 9–33.
- Flessa, K.W., 2001. Time-averaging. In: Briggs, D.E.G., Crowther, P. (Eds.), *Palaeobiology II*. Blackwell, Oxford, pp. 292–296.
- Flessa, K.W., Kowalewski, M., 1994. Shell survival and time-averaging in nearshore and shelf environments: estimates from the radiocarbon literature. *Lethaia* 27, 153–165.
- Flessa, K.W., Cutler, A.H., Meldahl, K.H., 1993. Time and taphonomy: quantitative estimates of time-averaging and stratigraphic disorder in a shallow marine habitat. *Paleobiology* 19, 266–286.
- Fürsich, F.T., Aberhan, M., 1990. Significance of time-averaging for paleocommunity analysis. *Lethaia* 23, 143–152.
- Goodfriend, G.A., Flessa, K.W., 1997. Radiocarbon reservoir ages in the Gulf of California: role of upwelling and flow from the Colorado River. *Radiocarbon* 39, 139–148.
- Goodwin, D.H., Flessa, K.W., Schöne, B.R., Dettman, D.L., 2001. Cross-calibration of daily growth increments, stable isotope variation, and temperature in the Gulf of California bivalve mollusk *Chione* (*Chionista*) *cortezii*: implications for paleoenvironmental analysis. *Palaios* 16, 415–426.
- Goodwin, D.H., Schöne, B.R., Dettman, D.L., 2003. Resolution and fidelity of oxygen isotopes as paleotemperature proxies in bivalve mollusk shells: models and observations. *Palaios* 18, 110–125.
- Grossman, E.L., Ku, T.L., 1986. Oxygen and carbon fractionation in biogenic aragonite: temperature effects. *Chemical Geology. Isotope Geoscience Section* 59, 59–74.
- Harding, B.L., Sangoyomi, T.B., Payton, E.A., 1995. Impacts of a severe sustained drought on Colorado River water resources. *Water Resources Bulletin* 31, 815–824.
- Hastings, J.R., 1964a. Climatological data for Baja California. Technical Reports on the Meteorology and Climatology of Arid Regions 14, 93.
- Hastings, J.R., 1964b. Climatological data for Sonora and northern Sinaloa. Technical Reports on the Meteorology and Climatology of Arid Regions 15, 104.
- Iribarne, O., Valero, J., Martinez, M.M., Lucifora, L., Bachmann, S., 1998. Shorebird predation may explain the origin of Holocene beds of stout razor clams in life position. *Marine Ecology. Progress Series* 167, 301–306.
- Keen, A.M., 1971. *Sea Shells of Tropical West America*. Stanford Univ. Press, Stanford, California.
- Keller, N., Del Piero, D., Longinelli, A., 2002. Isotopic composition, growth rates and biological behavior of *Chamelea gallina* and *Callista chione* from the Gulf of Trieste (Italy). *Marine Biology* 140, 9–15.
- Kidwell, S.M., Behrensmeier, A.K., 1993. Taphonomic approaches to time resolution in fossil assemblages. *Short Courses in Paleontology*, vol. 6. Paleontological Society, Knoxville.
- Kidwell, S.M., Bosence, D.W.J., 1991. Taphonomy and time-averaging of marine shelly faunas. In: Allison, P.A., Briggs, D.E.G. (Eds.), *Taphonomy, Releasing the Data Locked in the Fossil Record*. Plenum, New York, pp. 115–209.
- Kidwell, S.M., Flessa, K.W., 1995. The quality of the fossil record: populations, species, and communities. *Annual Review of Ecology and Systematics* 26, 269–299.
- Kowalewski, M., Goodfriend, G.A., Flessa, K.W., 1998. High-resolution estimates of temporal mixing within shell beds: the evils and virtues of time-averaging. *Paleobiology* 24, 287–304.
- Martin, R.E., 1999. *Taphonomy. A Process Approach*. Columbia Univ. Press, New York.
- Miller, A.I., 1988. Spatial resolution in subfossil molluscan remains: implications for paleobiological analysis. *Paleobiology* 14, 91–103.
- Rodriguez, C.R., Flessa, K.W., Téllez-Duarte, M.A., Dettman, D.L., Avila-Serrano, G.A., 2001. Macrofaunal and isotopic estimates of the former extent of the Colorado River estuary, Upper Gulf of California, México. *Journal of Arid Environments* 49, 185–189.
- Schöne, B.R., Goodwin, D.H., Flessa, K.W., Dettman, D.L., Roopnarine, P.D., 2002. Sclerochronology and growth of the bivalve mollusks *Chione flutifraga* and *Chione cortezii* in the northern Gulf of California, Mexico. *The Veliger* 184, 131–146.
- Shackleton, N.J., 1973. Oxygen isotope analysis as a means of determining season of occupation of prehistoric midden sites. *Archaeometry* 15, 133–141.
- Shackleton, N.J., 1986. The Plio–Pleistocene ocean: stable isotope history. In: Hsu, K.J. (Ed.), *Mesozoic and Cenozoic Oceans*. American Geophysical Union, Washington, DC, pp. 135–141.
- Springer, D.A., Flessa, K.W., 1996. Faunal gradients in surface and subsurface shelly accumulations from a recent clastic tidal flat, Bahia la Choya, northern Gulf of California, Mexico. *Palaeogeography, Palaeoclimatology, Palaeoecology* 126, 261–279.
- Thompson, R.W., 1968. Tidal flat sedimentation on the Colorado River delta, northwestern Gulf of California. *Memoir-Geological Society of America* 107, 1–133.